Application and Evaluation of Wavelet-based Surface Reconstruction for Contour Propagation in Radiotherapy

Stefano Moriconi[1], Elisa Scalco[1], Tiziana Rancati[2], Antonella Messina[3], Tommaso Giandini[4,5], Riccardo Valdagni[2,6], and Giovanna Rizzo[1]

[1]Institute of Molecular Bioimaging and Physiology (IBFM-CNR), Segrate (MI), Italy
{stefano.moriconi, elisa.scalco, giovanna.rizzo}@ibfm.cnr.it
[2]Prostate Cancer Program, Fondazione IRCCS Istituto Nazionale dei Tumori, Milan, Italy
{tiziana.rancati, riccardo.valdagni}@istitutotumori.mi.it
[3]Radiology Unit, Fondazione IRCCS Istituto Nazionale dei Tumori, Milan, Italy
antonella.messina@istitutotumori.mi.it
[4]Medical Physics Unit, Fondazione IRCCS Istituto Nazionale dei Tumori, Milan, Italy
[5]Radiotherapy Division, European Institute of Oncology, Milan, Italy
tommaso.giandini@istitutotumori.mi.it
[6]Dept. of Radiation Oncology1, Fondazione IRCCS Istituto Nazionale dei Tumori, Milan, Italy

Abstract. A wavelet-based open-source approach for three-dimensional (3D) surface reconstruction of anatomical structures, not yet used for radiotherapy (RT) applications, was presented. This was obtained from manual cross-sectional contours by combining both image voxel segmentation processing and implicit surface streaming methods using wavelets. 3D meshes reconstructed with the proposed approach were compared to those obtained from other three traditional triangulation algorithms. Evaluation was performed in terms of mesh quality metrics and accuracy of contour propagation in the pelvic district. Results have shown a smoothness and regularity of the reconstructed surface, comparable, or even better, than the other methods, and an accuracy of contour propagation in line with the state-of-art literature. This demonstrated the efficacy of the proposed approach for the 3D surface reconstruction in RT.

Keywords: surface reconstruction; wavelet; contour propagation; mesh quality

1 Introduction

An accurate and reliable organ representation is of great interest in Radiotherapy (RT), since dose planning, treatment evaluation and toxicity model are based on organ contours or organ volume. The availability of tomographic images acquired during the course of RT has opened the possibility to daily or weekly monitoring organ changes, thus improving the efficacy of the treatment taking into account these modifications. Deformable image registration combined with contour propagation methods are able to recover these spatial changes and to automatically recontour organs of interest. This approach was proposed by many authors [1-4]; however, not every work has described in detail the whole procedure. In general, contour propagation can be faced by deforming binary masks extracted from 2D contours [3], [4] or by deforming 3D surface meshes generated from 2D contours [1], [3]. In this last case, the choice of the method for the surface reconstruction has an impact on the final result: in fact, it is desirable to have regular and smoothed meshes for a good rep-

resentation of the organs of interest, in order to make some evaluation on the organs surface or volume (e.g. Dose Volume Histogram and Dose Surface Histogram) or to obtain an accurate contour propagation. However, the algorithm used to generate surface representation is not always described. Several studies in the past decades proposed different methods to obtain 3D surfaces from generic cross-sectional data, as, for example, marching cubes [5] and power crust [6]. Furthermore, licensed commercial software provide with automatic built-in tools for 3D surface reconstruction (e.g. Amira®, Mercury Systems, MA, USA). By using these approaches, acceptable results in terms of smoothness, regularization and mesh quality are not always obtained. Moreover, they can show a complex and time-consuming processing, which sometimes results in failure, especially with large and complex datasets, and, regarding commercial software, they are black-box or little is customizable about the surface reconstruction from contours.

In this work we proposed a different approach for 3D surface reconstruction of organs of interest from slice contours, based on wavelet [7], which theoretically provides smooth, accurate and interpolated 3D geometrical model of the organ, and which has not yet been proposed in RT applications. We compared it with other classical methods already used in this context [1], [8], [9], by evaluating them in terms of their intrinsic mesh quality and of accuracy of contour propagation. In this work we considered patients treated for prostate cancer and we focused on relevant structures of the pelvic district: the prostate itself, the bladder, the rectum and the penile bulb.

2 Materials and methods

2.1 Wavelet-based Surface Reconstruction (WSR).

Bi-dimensional (2D) manual contours are first mapped into binary voxel image segmentation. Since serial slice data is usually anisotropic, an optional inter-slice thickening step is used to obtain isotropic-like voxel segmentation of the structure. The inter-slice thickening step generates new slices between two adjacent ones by interpolating the binary segmentation using logical operators. The binary segmentation is then converted into a set of 3D oriented points in the physical-space coordinates. Each 3D oriented point, i.e. $\bar{p} = [x_p\ y_p\ z_p]$, is associated with its outward-pointing normal vector $\bar{n}$. The estimation of the 3D points' normals is determined by the cross product between the vectors joining the two closest points of $\bar{p}$ on the same slice and those on adjacent slices respectively. The set of normals is then normalized by the Euclidean norm. The outward-pointing direction is verified by evaluating the sign of the dot product between $\bar{n}$ and the vector joining $\bar{p}$ and the closest inner reference of the structure (i.e., the binary skeletonization), otherwise the direction of $\bar{n}$ is inverted accordingly. This step is performed in order to obtain a dense and homogeneous cluster of 3D oriented points which represents the discrete sampling of the surface to reconstruct. We refer to [10] for a more detailed description of the binary segmentation pre-processing step.

WSR algorithm is employed then to extract a 3D smooth, interpolated mesh of the structure from the cluster of oriented points. The algorithm, which is accurately described in [7], estimates an approximation of the solid structure by means of an indicator function (χ) using the input points. The algorithm constructs then an approximation of the original surface as the zero level-set of the indicator function itself. WSR algorithm can be summarized

in four sub-steps, namely, octree configuration, estimation of χ, smoothing χ and polygon generation. By configuring the octree, the multi-resolution spatial grid for estimating the indicator function is defined. It represents a hierarchical structure of maximal depth d_m that encodes subtrees to cells, corresponding to higher-resolution detail. The greater d_m, the finer the surface reconstruction. Limitations in d_m can be introduced by the finite allocable memory and by the intrinsic spatial resolution and extension of the structure's input points. The estimation of χ at each cell of the octree takes advantage of the multi-scale and hierarchical structure of the compactly supported wavelet basis. This allows an efficient representation of χ with a relatively small number of coefficients. By applying the divergence theorem, the wavelet coefficients are approximated over the input oriented points. The resulting indicator function χ is 0 outside the approximated solid structure, whereas it is 1 on the inside. The smoothness of χ depends on the choice of the wavelet basis. We adopted the Daubechies wavelet (D4) for the surface reconstruction. In general, as the support of the wavelet decreases, so it also does the smoothness of the reconstructed surface. To this purpose a further smoothing step is performed on the indicator function before extracting the surface mesh. It consists in pruning the isolated cells of the octree, and in filtering the octree with a convolution mask on adjacent cells. The convolution mask adopted is the tensor product of the mask (¼ ½ ¼) in $\mathbb{R}^3$. Lastly the polygonal (triangle) surface extraction is obtained by applying an octree contouring method [11] and eventually by running Marching Cubes [5], which is guaranteed to produce a water-tight topological and geometrical manifold. Adopted implementation: *http://josiahmanson.com/research/wavelet_reconstruct*

2.2 Dataset

T2-weighted MRI images acquired before and three months after RT were considered for five patients (MRI1 and MRI2, respectively). A set of 2D contours of prostate, bladder, rectum and bulb were manually drawn on each MRI study, consisting thus in a total set of 40 contours (i.e., 5 patients x 2 time-points x 4 structures). The choice of these four organs was justified by the need of testing methods on different conditions of size and amount of deformation. Surfaces were then generated from each set of 2D contours using the WSR method previously described and other three classical approaches already used in RT context, namely Marching Cubes (MCB) [5] combined with a Taubin non-shrinking filter [12], Power Crust (PWC) [6] and Amira surface generation (AMR) using the built-in *unconstrained* smoothing modality [13].

2.3 Image registration and contour propagation

MRI2 were mapped on the MRI1 using a non-rigid image registration method implemented in the open-source software Elastix [14]. The chosen registration method is the classical Free-Form Deformation based on B-splines [15], with the parameters optimization available in the Elastix implementation. In particular, Normalized Mutual Information was chosen as the similarity metric, the adaptive stochastic gradient descent was the adopted optimization algorithm, and by setting a sufficiently high number of iterations the registration is guaranteed to reach convergence. A multi-resolution approach in 5 steps was adopted, using a uniform control-points grid at each step; the final grid was made up by isometric cubes of 10 mm.

To automatically deform organs' contours of MRI1 on MRI2, a contour propagation method was adopted. The propagation procedure was integrated in the Elastix toolbox by applying the estimated deformation field on the vertices of the mesh generated from the 2D contours.

2.4 Mesh evaluation

The evaluation of the WSR method was carried out by comparing it with MCB, PWC and AMR algorithms. This comparison was done in terms of indices of mesh quality and accuracy of the contour propagation.

Mesh quality. The evaluation of WSR, MCB, PWC and AMR surfaces, before and after deformation, is here performed in terms of aspect ratio (AR) and curvature. AR quantifies the mesh quality by evaluating the regularity of each triangular element of the reconstructed surface relative to an optimal reference, i.e. the equilateral triangle [16]: the greater the AR, the worse the mesh quality. Curvature is a measure of the surface departure from planarity: meshes with smooth curvature have a more regular and realistic look. This was done by calculating the mean curvature of each vertex of the mesh [17] using the Kitware's open-source program ParaView (*www.paraview.org*).

Since in RT it is also of interest to have accurate and smoothed contours on 2D slices of the images, the reconstructed surfaces were cut on the plane of the correspondent MRI and contours were qualitatively evaluated.

Accuracy of contour propagation. In order to estimate the influence of the choice of the surface reconstruction method on contour propagation, accuracy was evaluated in terms of distances between the deformed mesh and the reconstructed surface from the originally delineated contours on MRI2. For this calculation, each deformed mesh was compared with the original one generated with the same method: i.e. WSR deformed surfaces were compared with surfaces reconstructed with WSR, and so on. Distances between surfaces were calculated as the Euclidean distance between every vertex point in the deformed mesh and the closest vertex point in the manual mesh. The same procedure was repeated inverting the reference surface and the mean (D_mean) and maximum (D_max) distances were stored.

3 Results

An exemplificative result of the four surface reconstruction methods and their effects on contour propagation is reported in Fig. 1, where the prostate is represented before and after deformation. WSR, MCB and AMR successfully generated all the surfaces, whereas PWC failed in 9 of 40 cases due to a non-reached convergence of the algorithm.

Mean percentage AR values for the prostate meshes and curvature of the four organs obtained using the considered methods are reported in Table 1 and Fig. 2, respectively. In the remaining three organs, values of AR had the same trend of the prostate and were not further reported.

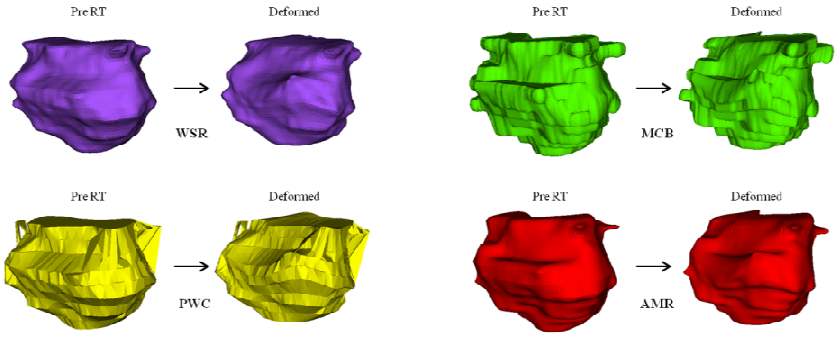

Fig. 1. Prostate surface reconstruction using the four described method starting from 2D contours (PreRT) and after deformation (Deformed). WSR: purple; MCB: green; PWC: yellow; AMR: red.

3.1 Mesh quality evaluation

Table 1. Values percentage's distribution of aspect ratio for the four methods in the prostate.

	Prostate AR percentage								
	1-10	**10-10^2**	**10^2-10^3**	**>10^3**		**1-10**	**10-10^2**	**10^2-10^3**	**>10^3**
WSR	0.96	0.04	0.00	0.00	**PWC**	0.63	0.17	0.08	0.13
MCB	1.00	0.00	0.00	0.00	**AMR**	0.99	0.01	0.00	0.00

As a general remark, the distribution of mean percentage AR for meshes obtained with WSR, AMR and MCB was limited to values in range 1-100, with more than 95% of triangles having an AR index lower than 10, thus meaning overall regular shape of the triangular elements. In particular, MCB showed the best performance, having the 100% of the triangles with AR lower than 10. Conversely, the AR percentage distribution of meshes obtained with PWC spans the whole range of values with a relatively greater amount of degenerate triangles (>35%). This was observed in original meshes as well as in propagated meshes, after the deformation process.

Even if MCB had the best AR, when surface curvature was observed, it showed a staircase effect, with anomalous curvature on the edges correspondent to slice changes; this did not happen with AMR and WSR, which had smooth and regular surfaces, with a planar mean curvature. PWC, which was already the worse method when AR was considered, deviated from planarity with a lot of vertices with anomalous curvature. This was verified on meshes generated from 2D contours as well as on deformed surfaces (Fig. 2).

2D contours obtained from the deformed prostate meshes were represented in Fig. 3, confirming what found in curvature. In fact it is possible to note that both AMR and WSR have a regular and smoothed shape, whereas PWC and MCB contours have an irregular look.

3.2 Accuracy of contour propagation

Results of accuracy of contour propagation are reported in Table 2.

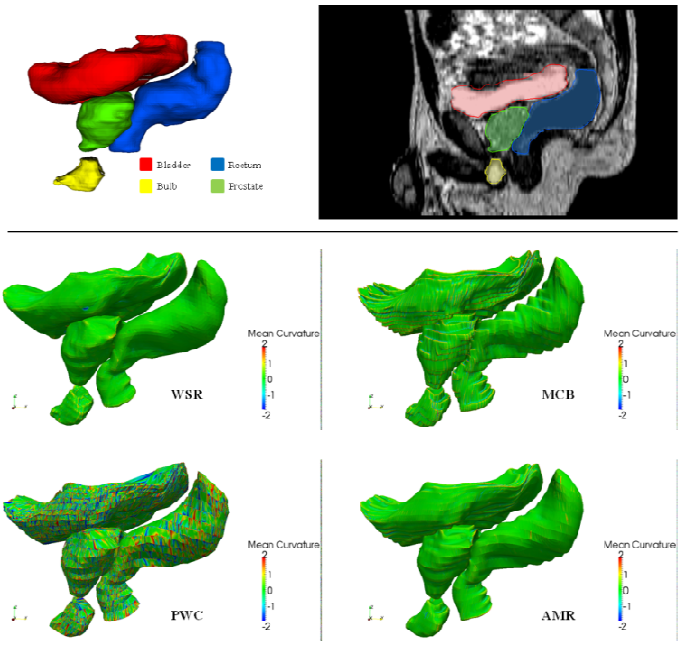

Fig. 2. Representation of the mean curvature of the deformed surfaces of the four organs, reconstructed with WSR, MCB, PWC and AMR. First row: model of the four organs and their area on a 2D sagittal plane.

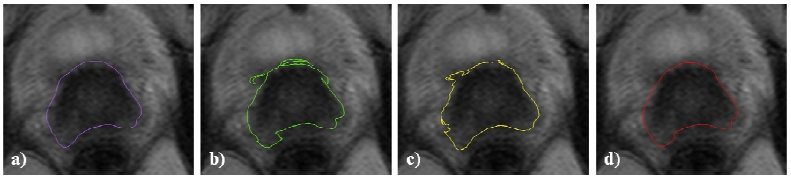

Fig. 3. A 2D representation of the deformed contours of the prostate on the correspondent T2w-MR image. a) WSR; b) MCB; c) PWC; d) AMR.

Among the four presented methods, PWC was the less robust, since it failed in numerous cases, thus preventing a successful contour propagation. For this reason, results of accuracy of PWC cannot be directly compared with the other methods and they were removed from Table 2. Regarding WSR, MCB and AMR, accuracy was quite different in bladder and bulb, whereas was practically the same in prostate and rectum. In general, WSR reported lower values of D_mean and D_max with respect to MCB and AMR.

4 Discussion and Conclusion

In this work a method based on wavelet was proposed to generate surfaces useful for contour propagation in RT; this method was compared with other three approaches already used in this context. Results have shown that globally the mesh quality and the accuracy of

Table 2. Accuracy of contour propagation in bladder, bulb, prostate and rectum using different surface reconstruction methods. Data are presented as mean ± st. dev. over the five subjects.

	D_mean [mm]	D_max [mm]	D_mean [mm]	D_max [mm]
	Bladder		**Prostate**	
WSR	1.65 ± 0.46	11.10 ± 3.33	1.59 ± 0.45	7.45 ± 2.56
MCB	1.55 ± 0.48	14.78 ± 6.65	1.57 ± 0.41	8.16 ± 2.47
AMR	1.80 ± 0.57	11.24 ± 3.02	1.62 ± 0.47	7.71 ± 2.44
	Bulb		**Rectum**	
WSR	1.18 ± 0.24	6.22 ± 2.35	1.95 ± 0.45	15.82 ± 5.24
MCB	1.27 ± 0.24	5.45 ± 1.77	2.19 ± 0.54	16.87 ± 5.04
AMR	1.42 ± 0.31	5.35 ± 1.67	2.19 ± 0.57	16.10 ± 6.19

contour propagation obtained with the proposed method are comparable, or even better, than the others.

Although all the considered approaches make use of intrinsically different smoothing paradigms, distinctive features and critical aspects of the resulting meshes are highlighted prior to deformation in terms of mesh quality. The analysis of mesh quality metrics has reported a very high shape regularity of the triangles of WSR and AMR surfaces; MCB, which presented the best values of AR percentages, revealed a staircase effect in curvature, not observable by the AR. It is likely that the staircase effect observed on MCB meshes can be reduced by introducing an anisotropic gaussian-smoothing kernel, however this would require a specific and ad-hoc tuning process of the pre-filtering step. PWC, presenting the worse yield both in AR and curvature, resulted in inadequate triangles. This suggests that surfaces reconstructed with WSR and AMR have a more regular lattice of the triangular mesh, resulting in more reliable organ surfaces.

The accuracy of contour propagation is comparable with other state-of-art works in the pelvic district [18], [19]. These results highlighted that the contribution of the registration error is larger than the effect of the surface reconstruction method, as can be noted from the quantitative analysis, where distances were similar over the considered methods. However, this second aspect has an impact on the final yield of the 2D deformed contours. In fact, as can be seen in Fig. 3, the MCB and PWC methods resulted in irregular contours, while WSR and AMR showed a smoothed shape. This is particularly true for bladder and prostate, whereas smoothed contours were found in rectum and bulb, due to a lower variability along the z-axis, which minimizes the staircase effect of the MCB.

Lastly, runtime performances showed similar values among the considered methods. Overall, a mean processing time of <1.0 s is observed for surface generation and mesh propagation together in each evaluated structure using the described configuration.

In conclusion, the WSR proposed method was able to generate qualitatively optimal surfaces, which can be used in the contour propagation framework with an accuracy in line with the state-of-art works. No limiting assumption, nor any ad-hoc tuning of the parameters is performed with the proposed approach. These results are comparable with those obtained with AMR; nonetheless, WSR has also the advantage of being open-source and can be easily integrated in Elastix.

Acknowledgements. The study was partially funded by "Ministero degli Affari Esteri e della Cooperazione Internazionale, Direzione Generale per la Promozione del Sistema Paese (MAECI - DGSP)". Fondazione Italo Monzino is acknowledged for supporting clinical research in prostate cancer. AIRC is aknowledged for supporting one of the authors (TG), grant AIRC N-14300.

References

1. Faggiano, E., Fiorino, C., Scalco, E. et al.: An Automatic Contour Propagation Method to Follow Parotid Gland Deformation during Head-and-Neck Cancer Tomotherapy. Phys. Med. Biol., **56** (2011) 775-791
2. Thor, M., Petersen, J. B., Bentzen, L. et al.: Deformable Image Registration for Contour Propagation from CT to Cone-Beam CT Scans in Radiotherapy of Prostate Cancer. Acta Oncol., **50** (2011) 918-925
3. Hardcastle, N., Tomé, W. A., Cannon, D. M. et al.: A Multi-Institution Evaluation of Deformable Image Registration Algorithms for Automatic Organ Delineation in Adaptive Head and Neck Radiotherapy. Radiation Oncology, **7** (2012) 90
4. Gu, X., Dong, B., Wang, J. et al.: A Contour-Guided Deformable Image Registration Algorithm for Adaptive Radiotherapy. Phys. Med. Biol., **58** (2013) 1889
5. Lorensen, W. E., & Cline, H. E.: Marching Cubes: A High Resolution 3D Surface Construction Algorithm. **21** (1987) 163-169
6. Amenta, N., Choi, S., Kolluri, R. K.: The Power Crust. (2001) 249-266
7. Manson, J., Petrova, G., Schaefer, S.: Streaming Surface Reconstruction using Wavelets. **27** (2008) 1411-1420
8. Deurloo, K. E., Steenbakkers, R. J., Zijp, L. J. et al.: Quantification of Shape Variation of Prostate and Seminal Vesicles during External Beam Radiotherapy. International Journal of Radiation Oncology* Biology* Physics, **61** (2005) 228-238
9. Wang, H., & Fei, B.: Nonrigid Point Registration for 2D Curves and 3D Surfaces and its various Applications. Phys. Med. Biol., **58** (2013) 4315
10. Moriconi, S., Scalco, E., Broggi, S. et al.: High Quality Surface Reconstruction in Radiotherapy: Cross-Sectional Contours to 3D Mesh using Wavelets. **In press** (2015)
11. Schaefer, S., & Warren, J.: Dual Marching Cubes: Primal Contouring of Dual Grids. **24** (2005) 195-201
12. Taubin, G., Zhang, T., Golub, G.: Optimal surface smoothing as filter design. Springer (1996)
13. Stalling, D., Zöckler, M., Sander, O. et al.: Weighted labels for 3D image segmentation. Konrad-Zuse-Zentrum für Informationstechnik Berlin (1998)
14. Klein, S., Staring, M., Murphy, K. et al.: Elastix: A Toolbox for Intensity-Based Medical Image Registration. Medical Imaging, IEEE Transactions on, **29** (2010) 196-205
15. Rueckert, D., Sonoda, L. I., Hayes, C. et al.: Nonrigid Registration using Free-Form Deformations: Application to Breast MR Images. Medical Imaging, IEEE Transactions on, **18** (1999) 712-721
16. Knupp, P. M.: Algebraic Mesh Quality Metrics for Unstructured Initial Meshes. Finite Elements Anal. Des., **39** (2003) 217-241
17. Dyn, N., Hormann, K., Kim, S. et al.: Optimizing 3D Triangulations using Discrete Curvature Analysis. Mathematical methods for curves and surfaces, **28** (2001) 135-146
18. Gardner, S. J., Wen, N., Kim, J. et al.: Contouring Variability of Human-and Deformable-Generated Contours in Radiotherapy for Prostate Cancer. Phys. Med. Biol., **60** (2015) 4429
19. Varadhan, R., Karangelis, G., Krishnan, K. et al.: A Framework for Deformable Image Registration Validation in Radiotherapy Clinical Applications. J. Appl. Clin. Med. Phys., **14** (2013) 4066